Multicolor Infrared Observations of SN 2006aj, the Supernova Associated with XRF 060218 - Paper I

Daniel Kocevski [1], Maryam Modjaz [2], Joshua S. Bloom [1], Ryan Foley [1], Daniel Starr [3], Cullen H. Blake [2], Michael Wood-Vasey [2], Emilio E. Falco [2], Nathaniel R. Butler [1], Mike Skrutskie [4], Andrew Szentgyorgyi [5]

kocevski@berkeley.edu, mmodjaz@cfa.harvard.edu, jbloom@astro.berkeley.edu, froley@astro.berkeley.edu, dstarr1@gmail.com, cblake@cfa.harvard.edu, wmwood-vasey@cfa.harvard.edu, efalco@cfa.harvard.edu, nat@astro.berkeley.edu, mfs4n@virginia.edu, saint@cfa0.cfa.harvard.edu

ABSTRACT

We report simultaneous multicolor near-infrared (NIR) observations of the supernova associated with x-ray Flash 060218 during the first 16 days after the high energy event. We find that the light curve rises and peaks relatively fast compared to other SN Ic, with the characteristic broad NIR peak seen in all three bands. We find that the rise profile before the peak is largely independent of NIR wavelength, each band appearing to transition into a plateau phase around day 10–13. Since the light curve is in the plateau phase when our observations end at day 16, we can only place limits on the peak absolute magnitudes, but we estimate that SN 2006aj is one of the lowest NIR luminosity XRF/GRB associated SNe observed to date. The broad peaks observed in the JHK_s bands point to a large increase in the NIR contribution of the total flux output from days 10–16. This evolution can be seen in the broad color and SED diagrams constructed using $UBVRIJHK_s$ monochromatic flux measurements for the first 16 days of the event. Ultimately, a 10-day rise time would make SN 2006aj an extremely fast rise SN Ic event, faster than SN 1998bw and SN 2003dh, which combined with its underluminous nature, indicates a lower amount of ^{56}Ni ejected

[1]Astronomy Department, University of California, 601 Campbell Hall, Berkeley, CA 94720

[2]Department of Astronomy, Harvard University, 60 Garden St., Cambridge, MA 02138

[3]Gemini Observatory, Hilo, HI 96720

[4]Department of Astronomy, P.O. Box 3818, University of Virginia, Charlottesville, VA 22903-0818.

[5]Harvard-Smithsonian Center for Astrophysics, Cambridge, MA 02138

by the progenitor compared to other XRF/GRB-SNe. Furthermore, the lack of significant color change during the rise portion of the burst points to little or no spectral evolution over the first 10 days of activity in the NIR.

Subject headings: gamma-rays bursts—Infrared: Observations

1. Introduction

There is now a growing body of evidence to suggest that most long duration, soft-spectrum gamma-ray bursts (GRBs) are associated with the core collapse of massive stars. This connection had long been suggested on theoretical grounds (Colgate 1968, Woosley 1993) as well as due to the similarities between GRB and SNe energetics. As of early 2006, this connection had been solidified by the detection of a total of three GRBs (GRB 980428/SN 1998bw, GRB 031203/SN 2003lw , and GRB 030329/SN 2003dh) with direct spectroscopic connections to supernova events. The early optical spectra of these supernovae components for which high-quality spectra exist show remarkable similarities, typically deficient of hydrogen and helium lines, a property consistent with Type Ic supernova. Furthermore, very broad absorption lines of O I, Ca II, and Fe II indicate high expansion velocities and a kinetic energy (E_K) going much higher than the values inferred in typical SN Ic events. Despite great interest in understanding the GRB-SN connections, only a few events have been observed well in the infrared (Lipkin et al. 2004; Cobb et al. 2006; Bloom et al. 2004). Since estimates of E_K and the amount of ^{56}Ni produced in the explosion depend on the total bolometric output, IR observations become particularly important for our understanding of the fundamental properties of these events.

On 2006 February 18 at 03:34:30 UTC the Swift spacecraft detected and localized XRF 060218 (Cusumano et al. 2006). The burst was immediately recognized as an unusual event when compared to other bursts observed by Swift. It was far longer than any GRB or XRF previously detected by the spacecraft, with a T_{90} duration of roughly 2000 seconds. It also exhibited a soft gamma-ray spectrum (Barbier et al. 2006) and an unusual afterglow that brightened for the first ten hours after the explosion before transitioning to a more common power law decay (Cusumano et al. 2006; Campana et al. 2006). The first indications of an underlying SN were noted by spectra taken roughly 3 days after the event (Masetti et al. 2006) followed by reports of a rebrightening of the optical counterpart shortly thereafter (D'Avanzo et al. 2006). Like previously observed XRF/GRB-SN the spectra of SN 2006aj showed continuum and broad-line emission with significant amounts of Fe II and Si II λ6355 but no H or He emission. The SN 2006aj spectra best matches those of SN 2002ap and SN 1997ef at similar epochs, both broad line SN Ic events but neither of which have been

conclusively shown to be associated with a XRF or GRB (Modjaz et al. 2006a). Emission line measurements by Mirabal et al. (2006) gave a redshift of $z = 0.0331$ making it one of the closest XRF/GRB ever observed, second only to GRB 980425. Such a close distance, ~ 140 Mpc, meant that XRF 060218 was similar to two other nearby XRF/GRB-SN events, GRB 980428 and GRB 031203, in that they were all significantly underluminous in the total amount of emitted gamma-ray, x-ray, and radio energies when compared to the majority of cosmological bursts (Soderberg et al. 2006). The V band peak of SN 2006aj occurred at roughly T = 10.0 days (9.7 days in the rest frame) with a peak apparent magnitude of $M_v = 18.7 \pm 0.2$ mag (Modjaz et al. 2006a; Sollerman et al. 2006; Mirabal et al. 2006), making it both the fastest evolving and least luminous of the XRF/GRB-SN observed to date. Pre-burst imaging of the SN 2006aj field by SDSS provided its host galaxy magnitudes (Cool et al. 2006; Hicken et al. 2006), which given its distance reveal a low-luminosity dwarf galaxy as the host, with low metallicity (Modjaz et al. 2006a), similiar to the majority of other GRB host galaxies (Stanek et al. 2006; Kewley et al. 2006).

PAIRITEL observations of XRF 060218/SN 2006aj started on Feb 20th, well before the observed V band and J band peaks reported by Modjaz et al. (2006a) and Cobb et al. (2006), and continued for the next 14 days. Here in Paper I we report on the light curve properties and host-subtracted absolute magnitudes of SN 2006aj in the J, H, and K_s infrared bands during these epochs. We reserve a more detailed presentation of the broadband SED evolution during this period for Paper II (Modjaz et al. 2006b). We present our observation and data reduction techniques and results in §2 and discuss the implications of our observations to the further understanding of the XRF/GRB-SN phenomena in §3.

2. Data & Analysis

All of the infrared data presented in this paper were taken with the fully automated PAIRITEL project [1] located on Mt. Hopkins in Arizona. The 1.3m telescope contains the three Near-Infrared Camera and Multi-Object Spectrometer (NICMOS3) arrays formerly of the 2MASS project (Skrutskie et al. 1995) to simultaneously read near infrared J, H, and K_s (1.2, 1.6, and 2.2 μm respectively) band images. Each image consists of a 256 x 256 array with a pixel scale of 2 arcsec/pixel and an integration time of 7.8 s per image. These individual images are dithered in order to correct for bad pixels, and mosaics are created by drizzling the images, producing a Nyquist-sampled image with a pixel scale of 1 arcsec/pixel. The telescopes entire operating software has been built on the Python program-

[1] http://www.pairitel.org

ming language and allows for autonomous operation which can be monitored and controlled remotely (Bloom et al. 2005) making it excellent for the followup of transient events.

Observations began of XRF 060218 on the morning of Feb 20th and continued until the object fell below our airmass limits some 16 days later. A total of > 9000 individual images were taken in the J, H, and K_s wavebands to produce a total of 96 reduced mosaics. The individual images were dithered through a predetermined pattern for a single epoch of observations and then reduced through a custom pipeline. Bias and sky frames for each image were produced by median-combining several dithered exposures before and after the frame, whereas archival frames were used for the bad-pixel masks and flat fields. The final mosaics were produced using a drizzle technique (Fruchter & Hook 1997) for each epoch and filter with an equivalent exposure time ranging between 2 and 30 minutes. The average exposure time of each mosaic generally increased as the object moved to higher air mass in subsequent nights. Of the 96 mosaics produced through the automated reduction pipeline, 3 were unusable due to poor transmission on three nights, leaving ~ 31 usable mosaics per filter.

A custom pipeline was used to perform photometry the final J, H, and K_s mosaics, using aperture photometry via the *Sextractor* package (Bertin & Arnouts 1996) and PSF photometry via the *NSTAR* routine in IDL to estimate the instrumental magnitudes of every objects in each mosaic. These values were then compared to the original 2MASS catalog of the same field for zeropoint determination of each reduced frame. Finally, an IDL routine was employed to produce a light curve for every stellar object in the field for a final relative calibration. The resulting median Δm variations in these stellar light curves allow for additional corrections to be made to the SN light curve that account for any errors in the zeropointing of the individual mosaics.

Overall, we find that the aperture and PSF fitting routines generally yield equivalent values for J, H, and K_s band mosaics. We ultimately chose to use aperture photometry with a floating aperture radius roughly equal to 1.5, 1.75, and 2.0 times the seeing (FWHM) for the J, H, and K_s bands respectively. These factors were empirically determined to maximize the signal to noise in each band and result in aperture radii roughly ranging from 3 to 5 pixels.

To account for the host galaxy contribution in the SN light curve, we employ a modified version of the ISIS image subtraction routine developed by Alard (2000). We revisited the XRF 060218 field nine months after our original observations to obtain deep template imaging of the host galaxy when the SN contribution was negligible. In all, we obtained an effective exposure of roughly 5.5 hours in the J, H, and K_s bands after co-adding several nights of imaging of the host galaxy. Using this late-time template, we were able to produce

residual images containing the flux contribution of the SN minus the host galaxy. In order to quantify of the error involved in this subtraction process, we inserted a series of fake stars into the original mosaics and tracked the changes in their known magnitude through each subtraction. The resulting variations in the fake star light curves are then accounted for in the final host subtracted SN light curve. We find that the host galaxy's flux contribution to the uncorrected SN light curve in most of the subtractions is roughly equal to the host magnitude found in the late time template imaging, indicating the that host galaxy can be treated as a point source at the resolution of our images. This allows us to subtract the host contribution in catalog space in order to reduce the scatter in the final SN light curve.

3. Results

Figure 5 shows our host-subtracted JHK_s light curves for SN 2006aj over the course of the first 16 days since the burst plotted in the observer frame, with the H and K_s bands shifted by 0.9 and 1.5 mag respectively for clarity. Each data point reflects the median average of all observations taken in a single night of observations. The error bars represent the 1 σ standard deviation about this median magnitude added in quadrature to the individual photometric measurement errors of a single mosaic. On nights in which only one mosaic was available, only the photometric error was used, which is most likely an underestimate of the true (statistical + systematic) error.

The characteristic broad peak of SN Ic events can be seen in all three bands, where the light curves flatten between day 10 and 13, with the K_s band peak being more uncertain due to a gap in the available data. Cobb et al. (2006) has reported on J band data peaking around day 17, just beyond our observability range, so we may miss the peak magnitude in J by a day. To estimate the peak magnitudes of our data set, we employ a spline fit to the light curve of each individual filter and measure apparent peak magnitudes of J: 16.76 $\pm$ 0.03, H: 16.65 $\pm$ 0.05, and K_s: 16.39 $\pm$ 0.21. Our estimate of the J band peak is consistent with the peak J band measurements made by Cobb et al. (2006) of the the SN and host of 16.65 $\pm$ 0.06 mag at day 17, one day after our last observation. Both the H and K_s bands are expected to peak after the J band, so the above values can only act as upper limits to the HK_s peak magnitudes. All three PAIRITEL bands appear to transition to the plateau phase at roughly the same time, with the J band possibly preceding the H and K_s bands. The Galactic line-of-sight extinction values for each of the bands, $A_J = 0.112$, $A_H = 0.071$, $A_{K_s} = 0.045$ (Schlegel et al. 1998), have been subtracted from the apparent peak magnitudes. Extinction from the host galaxy has been estimated by Guenther et al. (2006) through the measurements of the equivalent width (EW) of the Na I D lines along the line of sight. They find that most

of the extinction is attributable to our Galaxy with a visual Galactic extinction of $A_V = 0.39 \pm 0.02$ mag and a corresponding visual host frame extinction of $A_V = 0.13 \pm 0.01$ mag. If we assume a ratio of total-to-selective extinction of $R_V = 3.1$ (Cardelli, Clayton, & Mathis 1989), we estimate near infrared extinction values from the host galaxy of roughly $A_J = 0.035.$, $A_H = 0.022$, $A_{K_s} = 0.015$ mag, which is considerably less than the extinction due to the line of sight through our own Galaxy. Because the well-studied hosts (Vreeswijk et al. 2004; Jakobsson et al. 2003; Savaglio & Fall 2004; Watson et al. 2006; Butler et al. 2006) of both nearby and cosmological GRBs appear to have a lower dust-to-metal ratio than the Milky Way and probably flatter extinction laws, we also consider total-to-selective extinction values of $R_V = 2.0$ (5.0), which yield roughly $A_J = 0.035(0.035)$, $A_H = 0.024(0.022)$, $A_{K_s} = 0.015(0.015)$ mag. None of these values deviates significantly from the $R_V = 3.1$ assumption and the effects on the final light curves are within the error of our photometry. At a distance of ~ 141 Mpc ($z = 0.0335$, $H_0 = 72$ km s^{-1}, $\Omega_m = 0.3$, $\Omega_\Lambda = 0.7$) the peak absolute magnitude in J and the upper limit in H and K_s, taking into account both sets of extinction values, comes to J: -19.02 ± 0.03, H: -19.13 ± 0.05, and K_s: -19.39 ± 0.24. In this case, these values are not k-corrected due to the low redshift of the event. Photometry from the deep late time images gives the host galaxy's JHK_s apparent magnitudes J: 18.99 $\pm$ 0.16, H: 18.52 $\pm$ 0.22, and K_s: 18.73 $\pm$ 0.34, uncorrected for Galactic extinction. This represents 33.6%, 36.7%, and 27.8% of the J, H, and K_s flux contribution to the SN light curve at early times, respectively.

It should be noted that fits to the early X-ray data (Butler 2007) collected by the Swift spacecraft show evidence for excess X-ray absorption beyond that due to our Galaxy alone $N_{H,\mathrm{Galactic}} = 1.11 \times 10^{21}$ cm^{-2} (Dickey & Lockman 1990): $N_H = 2.9 \pm 0.5 \times 10^{21}$ cm^{-2}, at $z = 0.033$. Galactic extinction (Cardelli, Clayton, & Mathis 1989) and the Galactic A_V–N_H relation (Predehl & Schmitt 1995) would then imply the following absorption magnitudes in addition to the absorption by the Galaxy: $A_J = 0.51 \pm 0.07$, $A_H = 0.33 \pm 0.04$, $A_{K_s} = 0.21 \pm 0.03$. As mentioned above, GRB host galaxies tend to have lower dust to metals ratio than and probably extinction laws that deviate from that of the Galaxy, possibly explaining the discrepancy between the Na I D and N_H determined extinction values. Thus these results are not subtracted from our photometry stated above but should be considered as upper limits to the possible extinction from the host galaxy.

We compare the observer frame NIR light curve to the light curve behavior at optical wavelengths in Figure 5. Here we plot our JHK_s photometry along with $UBVRI$ measurements made by Mirabal et al. (2006) for the first 26 days of the event using the 1.3m and 2.4m MDM telescopes. Each of the individual light curves is connected with a cubic spline for clarity. The final Mirabal et al. (2006) photometry that we adopt for our light curve comparison is host-subtracted and extinction-corrected assuming apparent host magnitudes

of $U = 20.10$, $B = 20.41$, $V = 20.09$, $R = 19.91$, $I = 19.54$ and galactic extinction of $A_U = 0.77$, $A_B = 0.61$, $A_V = 0.47$, $A_R = 0.38$, and $A_I = 0.28$. The previously observed trend of broader light curves at longer wavelengths can be seen when comparing the turn over time in the shorter wavelengths compared to our JHK_s measurements. The detailed modeling of the light curve behavior and the time-dependent radiative transfer calculations required for a full understanding of this trend have been accomplished for the case of SNe Ia (Kasen 2006), but have yet to be done for SNe Ib/c and are beyond the scope of this paper. This increase in the NIR flux contribution at late times can be nicely seen in the color diagram shown in Figure 5. Here we display our host subtracted and extinction corrected J band photometry minus the $UBVRI$ data from Mirabal et al. (2006) and our HK_s PAIRITEL measurements. The gradual steepening of the color differences is a function of $\Delta\lambda_{\rm eff}$ between the two filters and quantifies the relative difference between the light curve decay rates at shorter wavelengths with respect to the NIR. When fit with a linear function such that $\Delta m = \Delta m_0 - st$, the individual color difference slopes s in Figure 5 are: $J{-}K_s$: -0.020 ± 0.012, $J{-}H$: -0.011 ± 0.008, $J{-}I$: -0.014 ± 0.006, $J{-}R$: -0.032 ± 0.005, $J{-}V$: -0.048 ± 0.005, $J{-}B$: -0.097 ± 0.0046, $J{-}U$: -0.143 ± 0.007 mags/day.

The color evolution properties can also be seen in the spectral energy distribution (SED) shown in Figure 5 constructed using this same broad band $UBVRIJHK_s$ photometry . We converted the $UBVRIJHK_s$ photometry to monochromatic flux values using Johnson-Morgan $f_{\nu,\rm eff}$ flux zeropoints from Fukugita et al. (1995) for the Mirabal et al. (2006) data set and the 2MASS $f_{\nu,\rm eff}$ flux zeropoints given in Cohen et al. (2003) for our PAIRITEL data. The figure shows several SED curves ranging from roughly 1.5 to 12 days after the Swift trigger as measured in the observer frame of the host galaxy; the individual SEDs are connected with a cubic spline for clarity. From the plot it can be seen that the shorter wavelength contribution to the bolometric flux of the SN emission is much higher near the onset of the event and steadily decreases after day 7 in the host frame (day ~ 9 in the observer frame). As a result, a broadening of the SED profile can also be seen at late times as the NIR contribution to the bolometric flux increases, consistent with the conclusions drawn from Figure 5. A much more detailed analysis and discussion of the evolution of the XRF 060218/SN 2006aj SED using our PAIRITEL observations in conjunction with optical *UBVr'i'* photometry taken with the Mt Hopkins 48-inch will be covered in Paper II (Modjaz et al., in prep).

It is difficult to quantify the amount, if any, of the infrared emission over the first 16 days that is a result of light echos, a scenario in which the dust in the vicinity of the burst progenitor absorbs and then reradiates the optical and UV emission from the explosion (Graham et al. 1983; Waxman & Draine 2000) This would occur at a distance greater than the radius R_c at which the dust grains are destroyed due to sublimation, roughly $R_c \sim$ 10-12 pc (Waxman & Draine 2000). If the dust at this distance has a characteristic equilibrium

temperature of ∼2300 K (the temperature above which the grains are destroyed), then the resulting reradiated light would peak at $\lambda \sim 2(1+z)\mu$m, where z is the redshift of the event, which at low z corresponds roughly to the K band (Reichart 2001). Although the prompt UV and optical emission along the line of sight could contribute infrared emission on any time scale, the majority of the reradiated light is expected to be delayed as emission arrives from higher latitudes. We conclude that this effect, if present, contributes very little to our overall photometry primarily because the large sublimation radius would make the peak in the reradiated light occur beyond our last observation on day 16. Furthermore, a time varying excess in the K_s would be expected if this effect were significant, which is not reflected in the SED.

4. Discussion

There is no significant evidence that any of the individual NIR JHK_s light curves observed with PAIRITEL peaks significantly faster than the others, although the H and K_s light curves are expected to peak after the J band which would occur outside of our observation window. Furthermore, the rise profile in the individual J, H and K_s bands before the peak appears to be largely independent of wavelength, with the light curve in each filter exhibiting roughly the same slope. This would make the chromatic rise time properties of SN 2006aj consistent with bolometric rise time results reported by Yoshii et al. (2003) for SN 2002ap and points to little or no spectral evolution in the NIR in the days preceding peak brightness. This can be seen in the color difference plot shown in Figure 5, which shows no significant trend in color evolution between the infrared wavelengths during the rise portion of the burst. Furthermore, the sharp V band peak reported by (Modjaz et al. 2006a; Sollerman et al. 2006; Mirabal et al. 2006) points to a relatively large increase in the NIR contribution to the total flux output after day ~ 10.

If we consider day 13 as being the onset of the NIR plateau phase of SN 2006aj, then the broad J band peak would occur several days after the peak in the V band, which is estimated at 9.7 days in the rest frame by Modjaz et al. (2006a). This would make our J band rise time consistent with the previously observed trend in most SNe, in which the optical peak precedes the infrared peak, as was the case with GRB 980425/SN 1998bw and SN 2003lw, both of which peaked 1.6 (Galama et al. 1998) and 5 (Malesani et al. 2004) days later in I band than in V band respectively. The observed flattening of the NIR as early as day 10 makes SN 2006aj the fastest of the XRF/GRB-SNe observed to date, being substantially shorter in rise time than both GRB 980425/SN 1998bw and GRB 030329/SN 2003dh (Galama et al. 1998; Matheson et al. 2003). The fast evolution and plateau seen in SN 2006aj is reminiscent

of the light curve properties of broad-lined SNe Ic (SNe Ic BL), highly energetic core collapse SNe, that show no association with GRBs. Two such events, SN 2002ap and SN 1997ef, have broad bolometric light curves where the latter is estimated to peak in $\sim 10-12$ days, assuming the explosion date inferred by Mazzali et al. (2002). Similiarly, our peak absolute magnitude of -19.02 ± 0.03 measured in J and -18.7 measured in V (Modjaz et al. 2006a; Sollerman et al. 2006; Mirabal et al. 2006) would make SN 2006aj the faintest of the XRF/GRB associated SNe, yet still brighter than the average broad-lined SN Ic. This can be seen in Figure 5, where the J and R band light curves of XRF 060218/SN 2006aj are plotted along the J and R band light curves of GRB 980425/SN 1998bw and SN 2002ap. Both the peak luminosity and rise time properties of SNe light curves are generally governed by the amount of ^{56}Ni produced in the explosion, leading many authors to conclude that the fast evolving and underluminous nature of SN 2006aj points to smaller amounts of ^{56}Ni compared to other XRF/GRB-SNe. Modeling by Mazzali et al. (2006a) estimates the ^{56}Ni mass produced by SN 2006aj to be roughly $0.2M_{\odot}$, compared to SN 1998bw and SN 2003dh which are thought to have produced roughly 0.38−0.45M and 0.45−0.65M respectively (Mazzali et al. 2006b). Yet, this low estimate of ^{56}Ni for SN 2006aj is still higher than the $\sim 0.09M_{\odot}$ estimated for the SN 2002ap SN Ic BL (Foley et al. 2003) which reflects the amount typical produced by normal core-collapse SNe such as SN 1987A and SN 1994I.

SN 2006aj was also peculiar in several other aspects. First, the measured peak spectral energy of the gamma-ray emission $E_{pk} = 4.9$ keV, where E_{pk} is the max of the νF_{ν} spectra and hence where most of the gamm-ray energy is radiated, is extremely soft. This is in comparison to the GRB counterparts of SN 1998bw, 2003dh and 2003lw, which all had E_{pk} values of roughly 55, 79, and 159 keV respectively. Furthermore, the modeling done by Mazzali et al. (2006a) estimates an explosion kinetic energy of $E_K \approx 2 \times 10^{51}$ erg and total ejected mass of $M_{ej} \approx 2M_{\odot}$, both of which are lower than the values estimated for the other SNe with associated GRBs, but yet on the high end of the distribution of these values when compared to normal SN Ic events. Considering these relatively low E_{pk}, E_K, and M_{ej} values along with the low luminosity and fast rise time, it becomes clear that GRB 060218/SN 2006aj was indeed a peculiar type of event. It is quite likely that SN 2006aj, with its low E_K and M_{ej} values, is an intermediate type of event. Extreme in many ways when compared to broad-line core-collapse SNe like SN 2002ap and 1997ef which emit little or no high energy emission, but rather weak when compared to previously observed XRF/GRB-SNe. Li et al. (2006) has recently quantified a previously observed trend that correlates a GRB's E_{pk} value and the peak luminosity of its SNe emission, and hence the produced ^{56}Ni mass. Using this correlation, he estimates that the E_{pk} values for SN 2002ap and 1997ef, if they had possessed an associated GRB, would have occurred in the VU, far below the range of what is considered a GRB or XRF. This of course is based on the assuming this correlation is real and not an

artifact of observational biases or source evolution. All of the SN 2006aj properties discussed above place it between the previously observed GRB-SNe sample and these low-luminosity and low estimated E_{pk} broad-lined events, possibly pointing to a continuous distribution of SN events that emit at increasingly higher energies.

One possible explanation for such a continuous distribution of gamma ray energies is that the soft-spectrum and low-luminosity events like XRF 060218 are due to off-axis observations of typical long-duration GRB-SNe (Yamazaki et al. 2003). Although this off-axis scenario was originally involked to explain the peculiar high energy properties of GRB-SNe like SN 1998bw, recent numerical simulations performed by Maeda et al. (2006) have shown that the viewing angle of asymmetric explosions would also have an effect on the observed luminosity and time of peak of the associated SNe. Through the use of 3D Monte Carlo simulations, the authors find that asymmetric SNe would appear to peak earlier when viewed at small θ from the z-axis of the explosion, this being due primarily to low and extended ^{5}6Ni densities in that direction. The resulting luminosity as seen in the z-direction is then boosted correspondingly because the photons can only diffuse out in this direction. This small θ scenario would then predict fast peaking, high luminosity, and high E_{pk} events which is inconsistent with the parameter distribution seen in XRF 060218 which has a distinctly fast time to peak but a remarkably low luminosity and E_{pk}. Another difficulty of the off-axis interpretation is that it would require a very large intrinsic total energy of roughly $\sim 10^{53}$ ergs, which would be inconsistent with the relatively low kinetic energy measurements made from radio observations (Soderberg et al. 2006) at late times when the jet collimation and/or SNe asymmetry should no longer be significant. Furthermore, the probability of seeing a jet off-axis goes down significantly with increasing θ_j resulting in inconsistent rate ratios between high and low energy events as noted by Cobb et al. (2006). Therefore, although off-axis models can be made to successfully explain the observed range of GRB/XRF energetics, the range of SN properties such as E_K, M_{ej}, the measurements of which are generally independent of collimation, suggest that viewing angle effects alone cannot account for the full diversity of XRF/GRB-SNe properties. On the other hand, the distribution of the intrinsic properties of the progenitor star that would lead to such a continuous distribution in the observed XRF/GRB-SNe properties is also not entirely clear. A qualitative correlation between the estimated progenitor mass and the resulting explosive energy seen among several broad-line and normal core-collapse SNe (Mazzali et al. 2002) points to a high initial stellar mass along with the progenitor's rotation rate, both of which would govern whether the jet associated with the GRB breaks out of the progenitor, as likely candidates. Future broad-band observations of intermediate events like SN 2006aj and SN 2002ap may be crucial to the examination of this distribution and our understanding of the nature of the GRB-SNe connection.

5. Acknowledgments

The Peters Automated Infrared Imaging Telescope (PAIRITEL) is operated by the Smithsonian Astrophysical Observatory (SAO) and was made possible by a grant from the Harvard University Milton Fund, the camera loan from the University of Virginia, and the continued support of the SAO and UC Berkeley. Partial support for PAIRITEL operations and this work come from NASA grant NNG06GH50G ("PAIRTEL: Infrared Follow-up for Swift Transients"). This work was conducted under the auspices of a DOE SciDAC grant (DE-FC02-06ER41453), which provides support to J. S. B.'s group. J. S. B. thanks the Sloan Research Fellowship for partial support. D.K. acknowledges financial supported through the NSF Astronomy & Astrophysics Postdoctoral Fellowships under award AST-0502502.

REFERENCES

Alard, C. 2000, A&AS, 144, 363

Barbier, L., et al. 2006, GRB Circular Network, 4780

Bloom, J., Starr, D., Blake, C., Skrutskie, M., Falco, E., 2006, ASPC, 351, 751B (astro-ph/0511842)

Bloom, J., et al. 2004, AJ, 127, 252B

Bertin, E. & Arnouts, S., 1996, A&AS, 117, 393B

Butler, N. 2007, accepted to ApJ (astro-ph/0604083)

Butler, N., et al. 2006, ApJ, 652, 1390

Campana, S. et al. 2006, Nature, 442:1008C

Cardelli , J., Clayton, G., & Mathis, J., 1989, ApJ, 422, 158

Cobb, B. E., Bailyn, C. D., van Dokkum, P. G., & Natarajan, P. 2006, ApJ, 645, L113

Cohen, M., Wheaton, Wm. A., Megeath, S. T. 2003, AJ, 126, 1090C

Cool, R. et al. 2006, GRB Circular Network, 4777

Cusumano, G. et al. 2006a, GRB Circular Network, 4775

Cusumano, G. et al. 2006b, GRB Circular Network, 4786

D'Avanzo, P. et al. 2006, GRB Circular Network, 4810

Dickey, J. M., & Lockman, F. J. 1990 ARA&A, 28, 215

Foley et al. 2003, PASP, 115, 1220F

Fukugita, M. et al 1995, PASP, 107, 945F

Fruchter, A., & Hook, R. N. 1997, Proc. SPIE, 3164, 120

Hicken, M. et al. 2006 GCN Circ. 161

Galama, T., Vreeswijk, P., Van Paradijs, J., Kouveliotou, C., Augusteijn, T., et al. 1998b. Nature 395:670-72

Galama, T. J., & Wijer, R. A. M. J. 2001, ApJ, 549, L209

Graham et al. 1983, Nature, 304:25

Guenther, E. W., Klose, S., Vreeswijk, P., Pian, E., & Greiner, J. 2006, GCN Circular 4863

Jakobsson, P., et al. 2003, A&A , 408, 941

Kasen, D., 2006, ApJ, 649, 939K

Kewley, L., et al. 2006, AJ, in press, (astro-ph/0609246)

Li-Xin Li 2006, Accepted by MNRAS (astro-ph/0608315)

Lipkin, Y., 2004, ApJ, 606, 381L

Maeda, K., Mazzali, P., Nomoto, K., 2006, ApJ, 645.1331M

Matheson, T., et al. 2003, ApJ, 599, 394M

Malesani, D., et al. 2004, ApJ, 609, L5

Masetti, N., Palazzi, E., Pian, E., Patat, F., 2006, GRB Circular Network, 4792

Mazzali, P. A., Deng, J., Maeda, K., et al. 2002, ApJ, 572, L61

Mazzali, P. A., Deng, J., Nomoto, K., et al. 2006, Nature, 442, 1018

Mazzali, P. A., et al. 2006b, ApJ, 645, 1323

Mirabal, N., et al. 2006, GRB Circular Network, 4792

Mirabal, N., et al. 2006, ApJ, 643L, 99

Modjaz, M., Stanek, K. Z., Garnavich, P. M., et al. 2006a, ApJ, 645, L21

Modjaz, M., et al. 2006 in prep

Predehl, P., & Schmitt, J. H. M. M. 1995, A&A, 293, 889

Reichart, D., 2001, ApJ, 554, 643

Savaglio, S., & Fall, S. M. 2004, ApJ, 614, 293

Sollerman, J. et al. 2006, A&A, 454, 503S

Schlegel, D. et al. 1998, ApJ, 500, 525

Skrutskie, M., et al. 2006, AJ, 131.1163S

Stanek, R. et al. 2006, ApJ submitted (astro-ph/0604113)

Soderberg, A., Kulkarni, S. R., Nakar, E., et al. 2006, Nature, 442, 1014

Tominaga, N. et al. 2005, ApJ, 633L, 97

Watston, D., et al. 2006, Submitted to ApJ (astro-ph/0510368)

, E., & Draine, B.T., 2000, ApJ, 537, 796

Woosley, S., Bloom, J., 2006, ARA&A 44, 507

Yamazaki, R., Daisuke, Y., Nakamura, T., 2003, ApJ, 594L, 79Y

Yoshii, Y. et al. 2003, ApJ, 592, 467

Vreeswijk, P. M., et al. 2004, A&A, 419, 927

Figure Captions

Fig. 1. - Color composite finding charts of the host galaxy (seen in SDSS pre-imaging; left) and SN 2006aj (seen in PAIRITEL; right). The SDSS image is made using r-, i, z-band images (Cool et al. 2006) and the IR image using J, H, K_s from stacked mosaics obtained on 3 March 2006 UT, near in time to the peak of the optical emission of the SN. North is up and East is to the left.

Fig. 2. - The J band (blue circles), H band (green square), and Ks band (red diamonds) aperture photometry light curve of XRF 060218/SN 2006aj after subtraction of the host contribution. The H and K_s band light curves have been shifted by -0.9 and -1.5 magnitudes respectively for clarity. The three light curves have been corrected for Galactic and host line of sight extinction. The error bars represent the quadrature sum of the photometric errors associated with all the mosaics produced in a single night of observations plus the 1 σ standard deviation about their median magnitude. A flattening of the light curves in all wavebands can be seen by Day 16.

Fig. 3. - Light curves of 14 2MASS stars in the same field as GRB 0602189/SN 2006aj. Final calibrations of the SN light curves were made by using the variations of these field stars about their median magnitude.

Fig. 4. - Our near infrared PAIRITEL light curves plotted along with $UBVRI$ data taken from Mirabal et al. (2006). A steady progression of wider light curves at longer wavelengths is clearly seen.

Fig. 5. - Color diagram showing the subtraction of the PAIRITEL J band and H and K_s band data as well as the Mirabal et al. (2006) $UBVRI$ photometry. The slope of the color differences becomes steeper with increasing $\Delta\lambda_{\rm eff}$, showing a large increase in the NIR contribution to the total bolometric flux output of the SN at later times.

Fig. 6. - A broad spectral energy distribution diagram produced by converting the JHK_s band data and the Mirabal et al. (2006) $UBVRI$ photometry into monochromatic flux values and plotted vs the effective frequency of that band pass, corrected for the redshift of the host galaxy. The NIR contribution to the total energy represented by the SED can be seen to increase at later times.

Fig. 7. - A comparison of the R and J band light curve properties of XRF 060218/SN 2006aj (PAIRITEL), GRB 980425/SN 1998bw (Galama et al. 1998), and SN 2002ap (Foley et al. 2003; Yoshii et al. 2003). We use the explosion date of January 28.9 (JD = 2452303.4) inferred by Mazzali et al. (2002) as the $t = 0$ time for SN 2002ap.

Figures

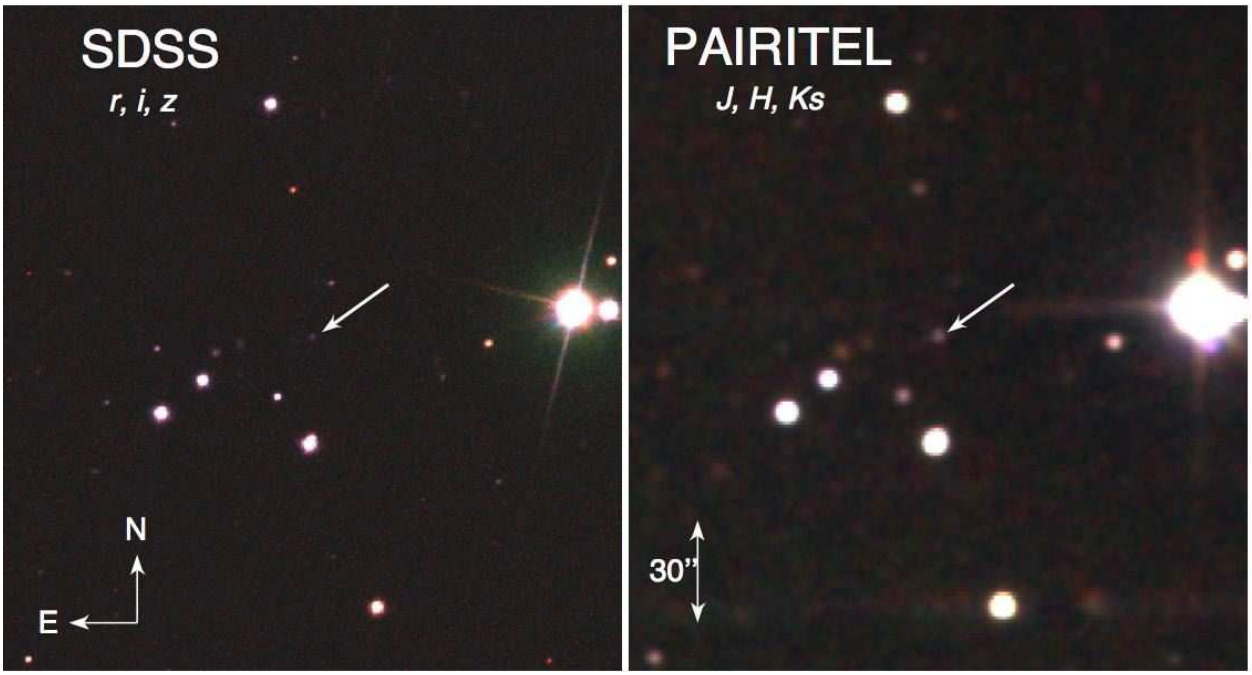
SDSS
r, i, z
N
E
PAIRITEL
J, H, Ks
30''

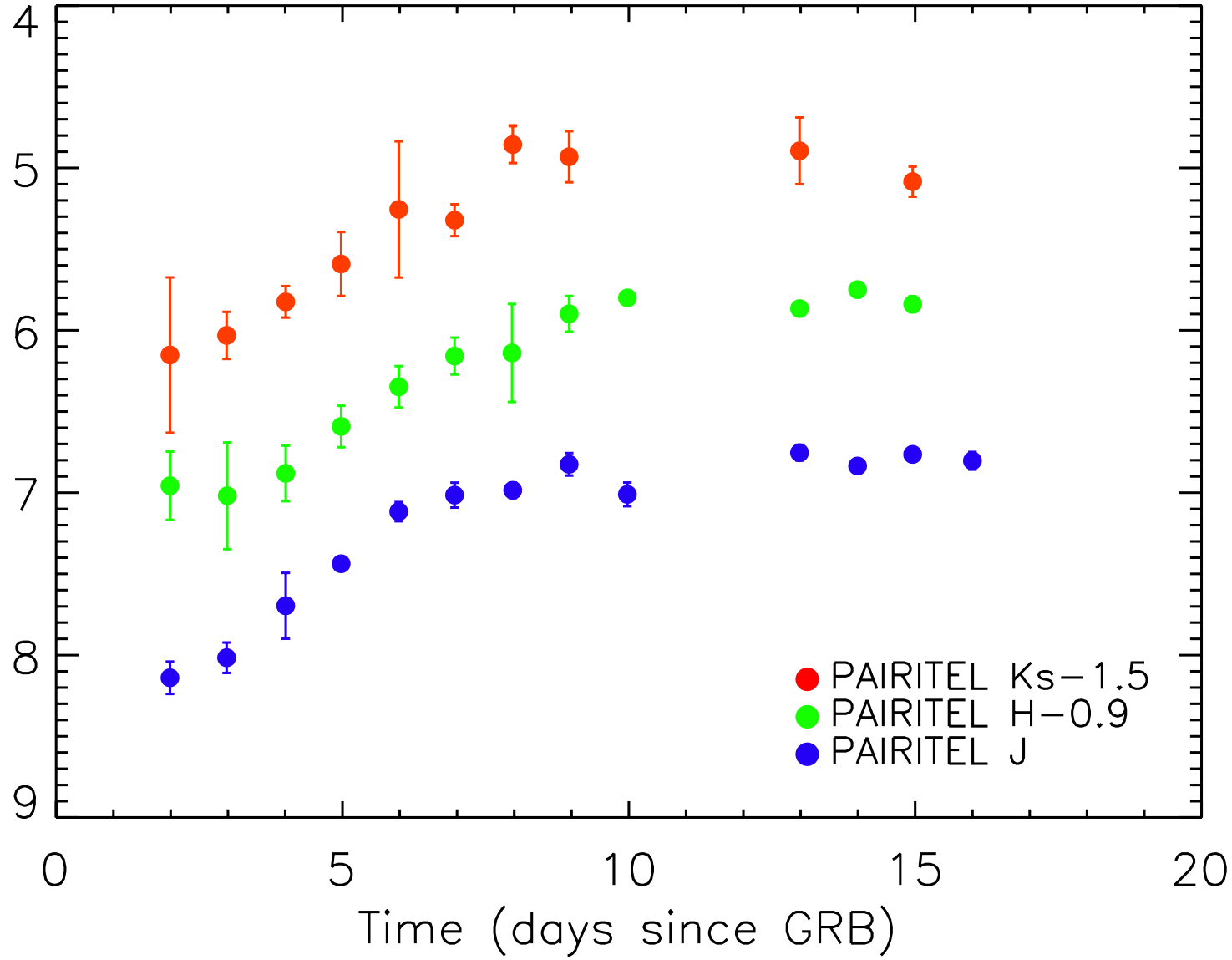
4
5
6
7
8
9
0
5
10
15
20
Time (days since GRB)
PAIRITEL Ks−1.5
PAIRITEL H−0.9
PAIRITEL J

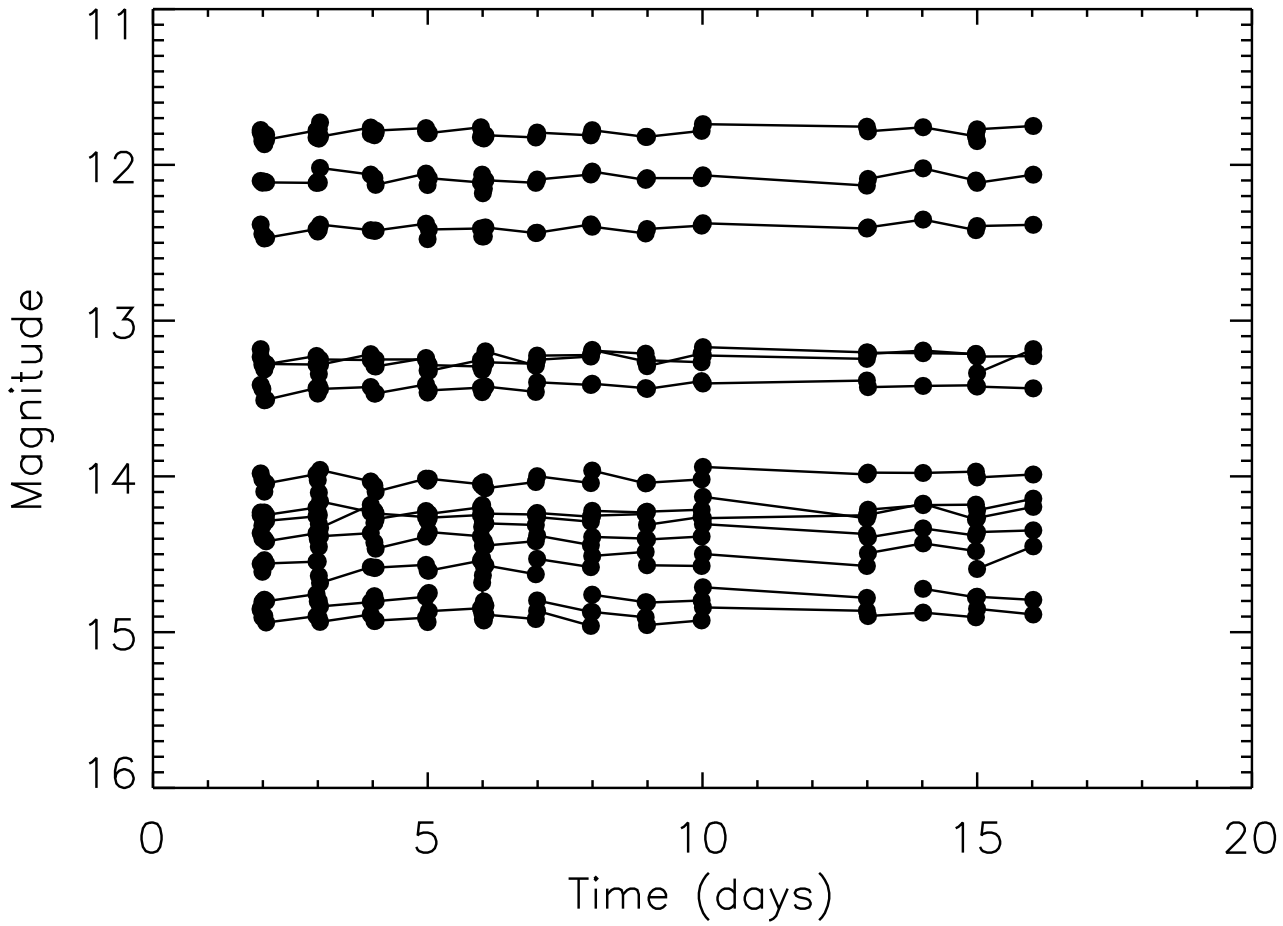
11
12
13
14
15
16
Magnitude
0
5
10
15
20
Time (days)

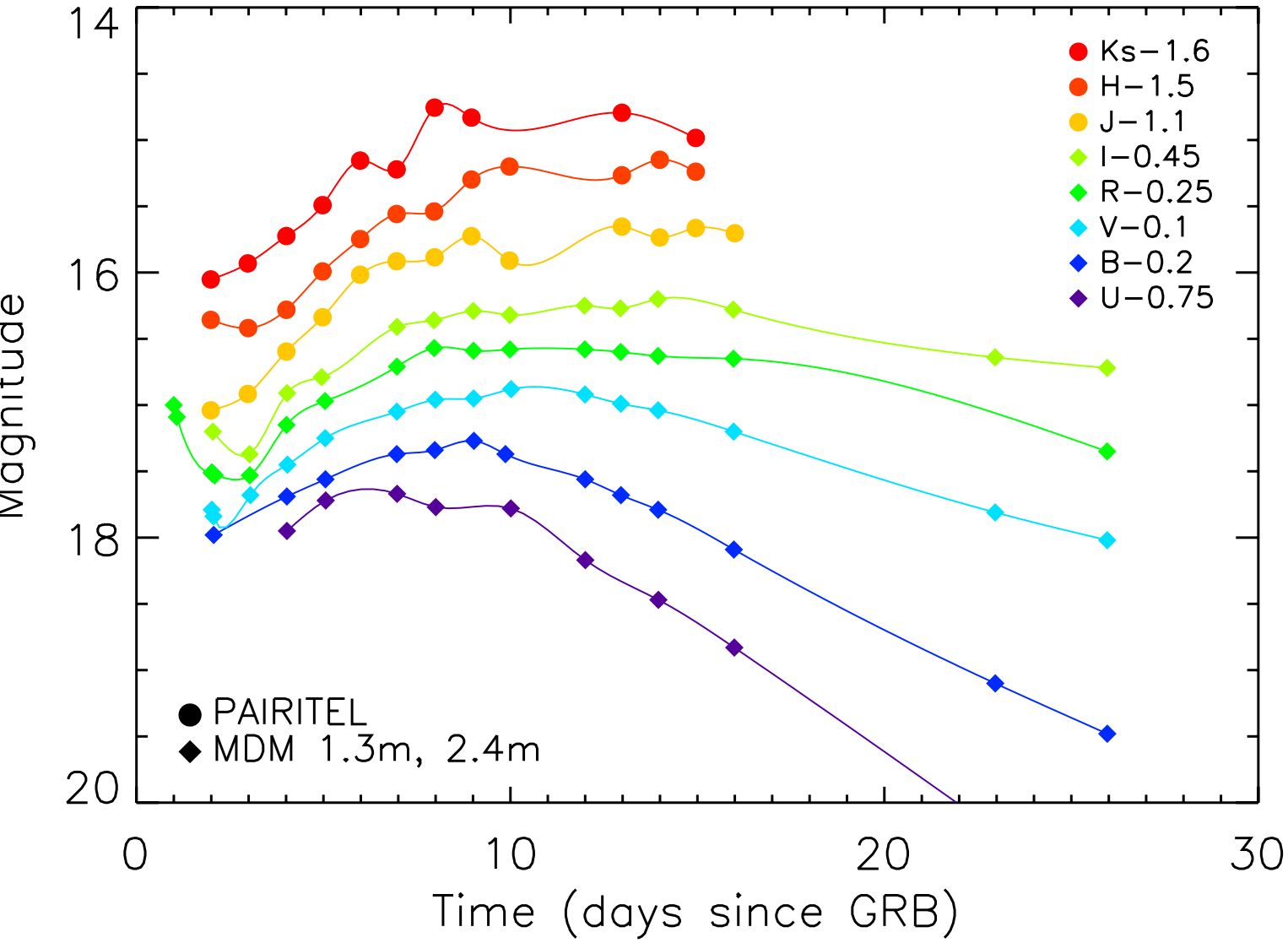
14
16
18
20
Magnitude
0
10
20
30
Time (days since GRB)
Ks−1.6
H−1.5
J−1.1
I−0.45
R−0.25
V−0.1
B−0.2
U−0.75
PAIRITEL
MDM 1.3m, 2.4m

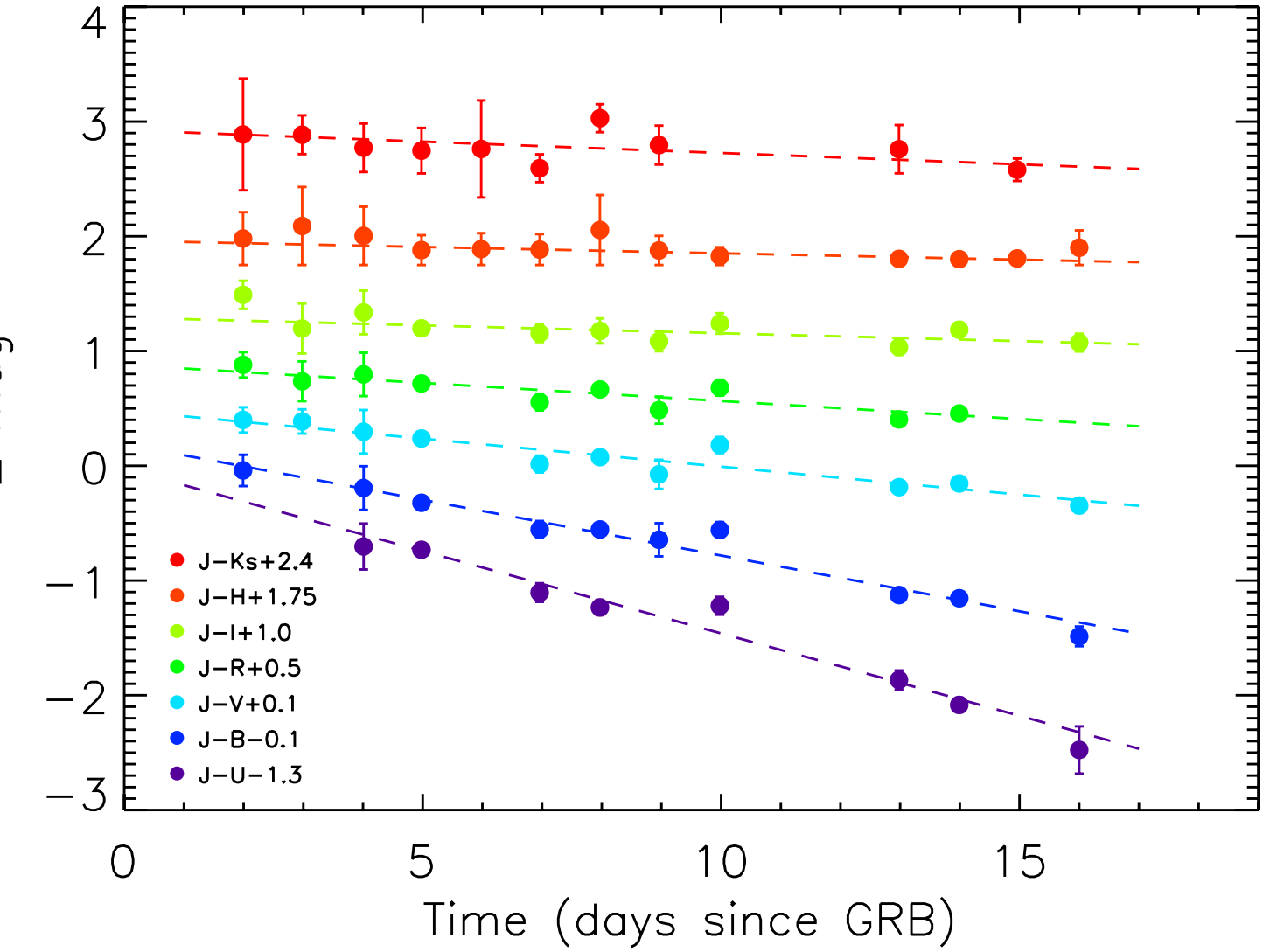
J−Ks+2.4
J−H+1.75
J−I+1.0
J−R+0.5
J−V+0.1
J−B−0.1
J−U−1.3
4
3
2
1
0
−1
−2
−3
0
5
10
15
Time (days since GRB)

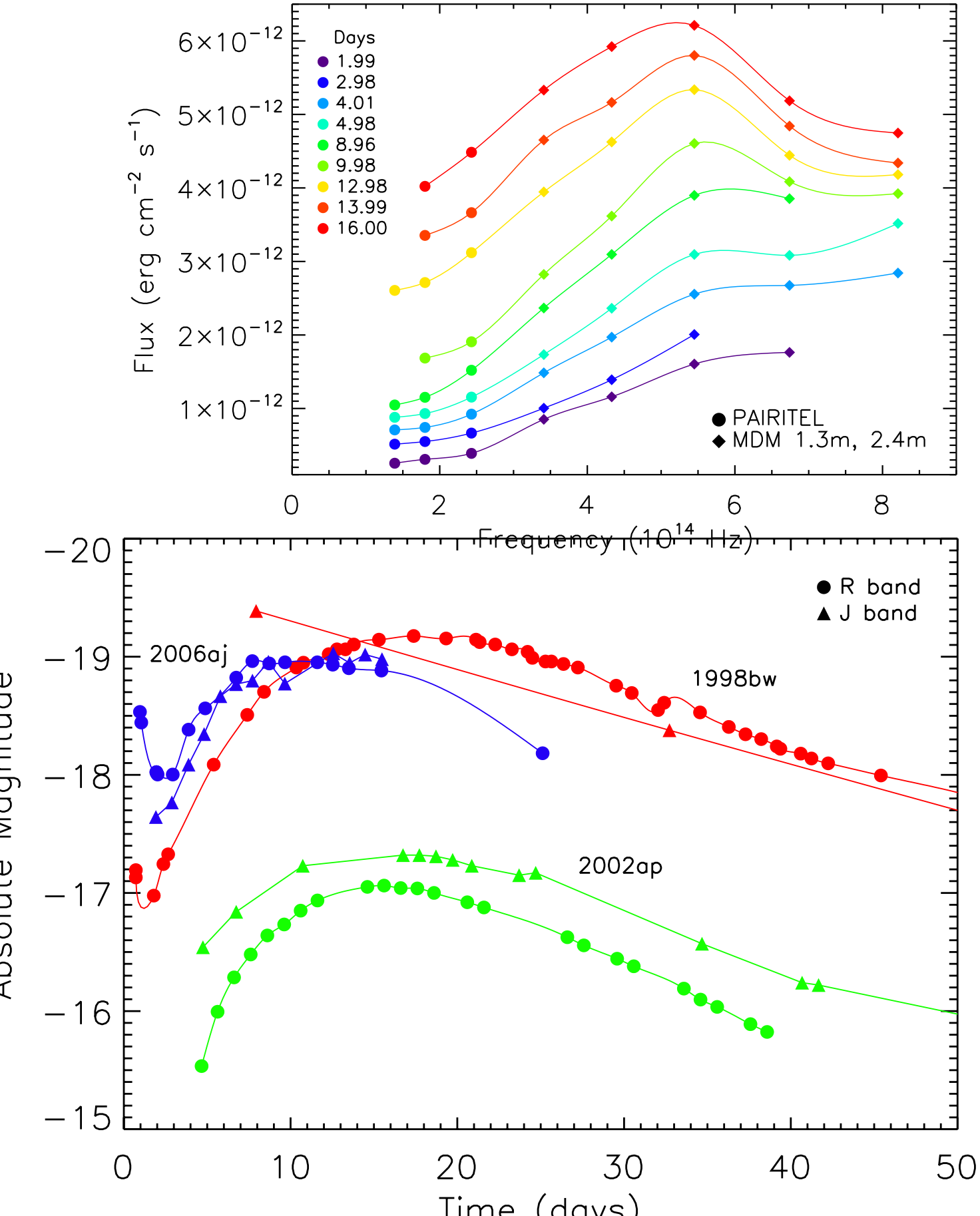
Days
1.99
2.98
4.01
4.98
8.96
9.98
12.98
13.99
16.00
PAIRITEL
MDM 1.3m, 2.4m
Flux (erg cm^{-2} s^{-1})
Frequency (10^{14} Hz)
R band
J band
2006aj
1998bw
2002ap
Absolute Magnitude
Time (days)

Table 1. Host Subtracted Photometry of XRF 060218/SN 2006aj

Days since GRB[1]	J band mag [2]	H band mag [2]	K_s band mag [2]	Seeing (arcsec)	Air Mass (sec z)
1.99	18.31 ± 0.09	17.97 ± 0.21	17.72 ± 0.48	2.93	1.10
2.98	18.18 ± 0.09	18.04 ± 0.33	17.26 ± 0.15	2.64	1.11
4.01	17.85 ± 0.19	17.89 ± 0.17	17.10 ± 0.10	2.76	1.20
4.98	17.58 ± 0.02	17.59 ± 0.13	16.91 ± 0.20	2.77	1.22
5.98	17.25 ± 0.05	17.34 ± 0.13	16.63 ± 0.42	2.89	1.32
6.96	17.15 ± 0.07	17.15 ± 0.11	16.69 ± 0.10	2.85	1.32
7.97	17.12 ± 0.04	17.13 ± 0.30	16.28 ± 0.11	2.92	1.43
8.96	16.96 ± 0.06	16.89 ± 0.11	16.35 ± 0.16	2.95	1.29
9.98	17.14 ± 0.07	16.79 ± 0.04		2.85	1.29
12.98	16.88 ± 0.04	16.85 ± 0.03	16.32 ± 0.21	1.45	1.21
13.99	16.97 ± 0.02	16.73 ± 0.05		2.82	1.22
14.96	16.89 ± 0.03	16.83 ± 0.05	16.48 ± 0.09	2.64	1.39
16.00	16.93 ± 0.05			2.83	1.37

[1]Observer frame

[2]Uncorrected for extinction

Table 2. XRF 060218/SN 2006aj Properties

Property	J band mag[1]	H band mag[1]	K_s band mag[1]
Peak mag	16.76 ± 0.03	$\lesssim 16.65 \pm 0.05$	$\lesssim 16.39 \pm 0.21$
Peak Mag[2]	-19.02 ± 0.03	$\lesssim -19.13 \pm 0.05$	$\lesssim -19.39 \pm 0.24$
Host mag	18.99 ± 0.16	18.52 ± 0.22	18.69 ± 0.34
$A_{galactic}$	0.112 ± 0.003	0.071 ± 0.002	0.045 ± 0.001
A_{host}[2]	0.035 ± 0.003	0.022 ± 0.002	0.015 ± 0.001

[1]Host subtracted and extinction corrected values

[2]$z = 0.0335$, $H_0 = 72$ km s^{-1}, $\Omega_m = 0.3$, $\Omega_\Lambda = 0.7$

[3]$R_V = 3.1$

Table 3. XRF 060218/SN 2006aj Absolute Magnitudes

Days since GRB[1]	J band mag[2,3]	H band mag[2,3]	K_s band mag[2,3]
1.92	-17.64 ± 0.09	-17.92 ± 0.21	-18.13 ± 0.49
2.88	-17.76 ± 0.09	-17.86 ± 0.33	-18.25 ± 0.15
3.88	-18.08 ± 0.19	-18.00 ± 0.17	-18.45 ± 0.10
4.81	-18.34 ± 0.03	-18.29 ± 0.13	-18.69 ± 0.22
5.79	-18.66 ± 0.06	-18.53 ± 0.14	-19.02 ± 0.48
6.73	-18.76 ± 0.08	-18.72 ± 0.13	-18.96 ± 0.11
7.71	-18.79 ± 0.05	-18.74 ± 0.33	-19.42 ± 0.14
8.67	-18.95 ± 0.07	-18.98 ± 0.12	-19.35 ± 0.19
9.65	-18.77 ± 0.07	-19.08 ± 0.04	
12.56	-19.02 ± 0.05	-19.01 ± 0.03	-19.38 ± 0.24
13.54	-18.94 ± 0.02	-19.13 ± 0.05	
14.47	-19.01 ± 0.03	-19.04 ± 0.06	-19.19 ± 0.11

[1]Rest frame of GRB

[2]Host subtracted and extinction corrected values

[3]$z = 0.0335$, $H_0 = 72$ km s^{-1}, $\Omega_m = 0.3$, $\Omega_\Lambda = 0.7$